

Channel Characteristic and Transmission Performance of An Indoor Wireless Optical Communication System

Chuan Peng and Jae Kyung Pan

Department of Electrical Engineering, Chonbuk National University
664-14 1Ga Deokjin-dong Jeonju, Jeonbuk 561-756, Korea
E-mail: chuan@chonbuk.ac.kr, pan@chonbuk.ac.kr

Abstract: Channel characteristics of an indoor wireless optical communication system is provided here. A channel impulse response includes the power ratio and time delay due to bounce times. Based on the scenario of the indoor structure, we obtained and discussed the received power distribution according to six configurations in Table 1, which vary with respect to transmitter and receiver positions and reflection coefficients. We used the input Gaussian pulse, Rectangular pulse, and Practical pulse, which are applied to pulse position modulation (PPM) and OOK, based on the impulse response of indoor channels in Configuration D. We evaluated the BER with respect to the signal-to-noise ratio per bit for various input pulses in line-of-sight (LOS) and diffuse channels.

1. Introduction

Wireless infrared communications via infrared radiation provide inexpensive, high speed data links for portable computer networks and have provoked great interest [1]. In an indoor IR wireless channel, the main concerns are both the total amount of received power and the time distribution.

In this paper we design simulated scenarios of various room conditions (ie. reflection coefficients of walls, radiation pattern mode, position of receiver, room size etc.). We investigated the simulation, to obtain the impulse response of a diffuse channel, and analyzed the scenario of the indoor structure we designed for the room structure shown in Fig. 1. Simulation results of the impulse response include the power ratio and time delay due to bounce times. We obtained and discussed the received power distribution, according to the six configurations in Table 1, which vary with respect to transmitter and receiver positions and reflection coefficients of the indoor structure [2].

Based on the channel impulse response, we investigate transmission performances of *L*-PPM with respect to input pulse shapes. We used the impulse response of LOS and diffuse channels. The input data of Fig. 2 is based on an input Gaussian pulse, Rectangular pulse, and Practical pulse, which are applied to *L*-PPM and OOK. To evaluate the transmission performance of *L*-PPM, we obtained the BER with respect to the signal to noise ratio for various input pulse shapes in LOS and diffuse channels.

This paper is organized as follows. Section 2 introduces the models of an indoor optical system and modulation schemes. In section 3, we present the simulation and analysis results using the input Gaussian pulse, Rectangular pulse, and Practical pulse, which are applied to *L*-PPM and OOK, and compare the BER performance in LOS and diffuse indoor links. Section 4 shows the conclusion.

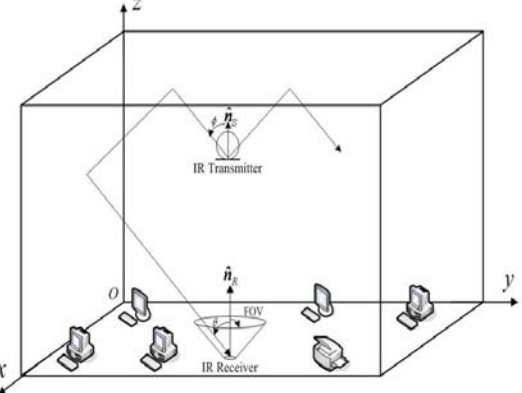


Fig. 1 Room structure and diffuse indoor infrared channel model.

2. Indoor Wireless Optical Communication System

2. 1 Channel model

A wide-beam optical source can be represented by a position vector \mathbf{r}_S , a unit-length orientation vector $\hat{\mathbf{n}}_S$, a power P_S , and a radiation intensity pattern $R(\phi, \theta)$, defined as the optical power per unit solid angle emitted from the source at position (ϕ, θ) with respect to $\hat{\mathbf{n}}_S$. The source radiance is given by [3]:

$$R(\phi) = \frac{n+1}{2\pi} P_S \cos^n(\phi) \quad \text{for } \phi \in [-\pi/2, \pi/2] \quad (1)$$

where n is the number of modes present in the source. The definitions and the channel model are shown in Fig. 1.

To simplify the notation, a point source S that emits a unit impulse of optical intensity at time zero is denoted by an ordered three-tuple:

$$S = \{ \mathbf{r}_S, \hat{\mathbf{n}}_S, n \}$$

where \mathbf{r}_S is the position, $\hat{\mathbf{n}}_S$ is the orientation, and n is the mode number. Linearity enables us to consider only unit-impulse sources, and scale the results for other sources. Similarly, a receiving element R with position \mathbf{r}_R , orientation $\hat{\mathbf{n}}_R$, area A_R , and Field Of View (FOV) is denoted by an ordered four-tuple:

$$R = \{ \mathbf{r}_R, \hat{\mathbf{n}}_R, A_R, \text{FOV} \}$$

Reflectors are assumed to be purely diffused and also ideal Lambertian.

Given a particular source S , and receiver R , in a room with reflectors, light from the source reaches the receiver after any number of reflections. Therefore, the impulse response is formulated as an infinite sum [3]:

$$h(t; S, R) = \sum_{k=0}^{\infty} h^{(k)}(t; S, R) \quad (2)$$

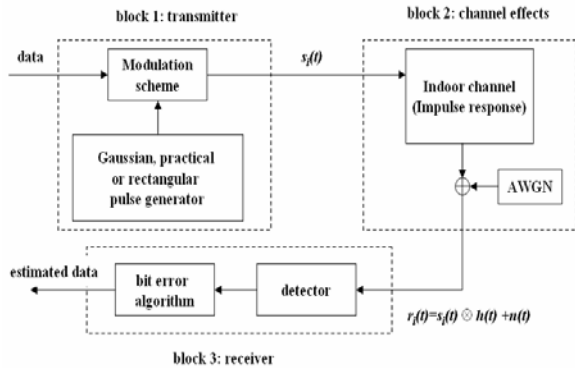


Fig. 2 Block diagram for transmission performance simulation of wireless optical communication system.

where $h^{(k)}(t)$ is the impulse response of the light undergoing exactly k and line of sight response

$$h^{(0)}(t; S, R) = \frac{n+1}{2\pi} \cos^n(\phi) d\Omega \text{rect}(\theta/\text{FOV}) \delta(t - R/c) \quad (3)$$

The higher-order terms ($k > 0$) are calculated recursively, as shown below:

$$\begin{aligned} h^{(k)}(t; S, R) &= \int_S h^{(0)}(t; S, \{r, \hat{n}, \pi/2, dA\}) \otimes h^{(k-1)}(t; \{r, \hat{n}, 1\}, R) \frac{\rho_i \cos^n(\phi) \cos(\theta)}{R^2} \\ &= \int_S \frac{n+1}{2\pi} \sum_{i=1}^N \rho_i \cos^n(\phi) \cos(\theta) \text{rect}(2\theta/\pi) h^{(k-1)}(t - R/c; \{r, \hat{n}, 1\}, R) \Delta A \end{aligned} \quad (4)$$

where the symbol denotes convolution. $h^{(k)}(t)$ can be approximated by:

$$\begin{aligned} h^{(k)}(t; S, R) &\approx \sum_{i=1}^N h^{(0)}(t; S, E_i) \otimes h(t; E_i, R) \\ &= \frac{n+1}{2\pi} \sum_{i=1}^N \rho_i \cos^n(\phi) \cos(\theta) \text{rect}(2\theta/\pi) h^{(k-1)}(t - R/c; \{r, \hat{n}, 1\}, R) \Delta A \end{aligned} \quad (5)$$

where E_i signifies the i -th and N is the total number of elements.

Characteristics of intensity modulation with direct detection infrared channels can be summarized in a simple form [4]:

$$r(t) = s(t) \otimes h(t) + n(t) \quad (6)$$

The received photocurrent $r(t)$ is the convolution of the transmitted optical power $s(t)$ and the channel impulse response $h(t)$. The $n(t)$ is modelled as an additive white

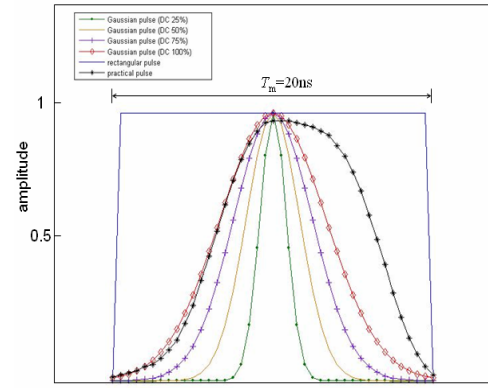


Fig. 3 Shape of various pulses: Practical, Rectangular and Gaussian with various duty cycles.

Gaussian noise (AWGN). Fig. 2 is a block diagram for transmission performance simulation; it describes the process of a modulated signal traversing the indoor channel and being received.

2.2 Modulation scheme

In our system (Fig. 2), we selected Gaussian, practical and rectangular pulses, to apply PPM and a traditional OOK scheme. The Gaussian waveform is a Gaussian pulse formulated as

$$g(t) = K e^{-(t/\tau)^2} \quad (7)$$

where $-\infty < t < \infty$, τ is a time-scaling factor and K is a constant. The parameter τ determines the shape of the waveform, so we obtain different Duty Cycles (DCs) of Gaussian pulses. Here, we select various typical pulses; Gaussian pulses with DCs varying between 25% and 100%. Other pulses are shown in Fig. 3; a practical pulse obtained from a function generator and an ideal rectangular pulse.

In the L -PPM scheme, to define a basis pulse with arbitrary shape $p(t)$, we modulate the data by delaying parameter τ_i to create pulses $s_i(t)$, as shown in Eq. (8).

$$s_i(t) = p_i(t - \tau_i) \quad (8)$$

Assuming an interval of duration T is divided into L sub-intervals, each $p_i(t)$ includes one slot of duration $T_S/L = T_m$, where T_S is the interval of duration and T_m is the time of the pulse slot.

In order to get the BER performance when different

Table 1 Indoor structure scenario for simulation.

Parameter \ Configuration	A	B	C	D	E	F	G
room	length(x)	6	6	6	6	6	variable
	width(y)	4	4	4	4	4	variable
	height(z)	3	3	3	3	3	variable
	ρ (4walls, ceiling, floor)	0.5	variable	0.5	0.5	0.5	0.5
transmitter	mode	1	1	variable	1	3	3
	x	3	3	3	3	3	3
	y	2	2	2	2	2	2
	Z	2.5	2.7	2.7	variable	2.5	2.5
receiver	area	1cm ²					
	FOV	70°	70°	70°	70°	70°	70°
	x	0.5	3	3	3	variable	3
	y	0.5	2	2	2	variable	2
	Z	0.5	1	1	1	variable	1

input pulses are applied to L-PPM and OOK, the pulses in Fig. 3 are utilized in the simulation.

3. Simulation and Analysis Results

The impulse response includes power ratio and time delay due to bounce times description of the channel characteristic of indoor optical communication system. To find the channel characteristics of an indoor wireless infrared communication system, we investigated the simulation, to obtain the impulse response of diffuse channels, and analyzed the scenario of the indoor structure we designed in Table 1. As shown in Table 1, the simulation was conducted in a room with three dimensional structure of 6 m (length) \times 4 m (width) \times 3 m (ceiling height). To design different configurations, we varied the rooms' reflection coefficients, transmitter parameters (i.e. position, pattern mode), and receiver parameters (i.e. position, FOV) etc.

In this scenario for simulations; in Configuration A, the configuration parameters are held constant. The impulse response of Configuration A is shown in Fig. 4. The power is decreasing for the higher-order impulse response in a diffuse channel. In Configuration B, we varied the reflection coefficients of the room between 0.1 and 0.8, as shown in Fig. 5. The simulation result in Configuration B shows that the higher the reflection coefficient, the higher the power received, as we expected. In this case, we assumed that the reflection coefficients of the four walls, the ceiling, and the floor are identical. In Configuration C, the source radiation pattern mode is varied between 1 and 50. The proper reflection coefficients of 0.5 are selected based on the simulation results for Configuration B and common sense. Fig. 6 shows that the highest received power is at $n=3$. The higher the value of n (where $n>3$), the lower the received power. In Configuration D and E, we obtain the received power ratio with respect to radiation patterns and transmitter heights. Fig. 7 shows that the highest received power level is at the radiation pattern of $n=3$ and height of 2.5 m. In Configuration F, we tested a mobile receiver located at four different points in the room.

$$[x, y, z] = [3, 2, 1], [1, 2, 1], [2, 2, 1], [1, 1, 1]$$

The received power ratio for the four different points are - 107.0 dB, - 122.9 dB, - 111.8 dB and - 125.9 dB.

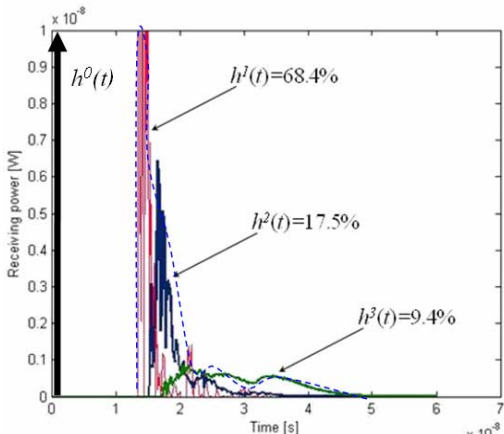


Fig. 4 Impulse response for light undergoing $k \in \{0, 1, 2, 3\}$ reflections.

And, the simulation result of Configuration G with respect to room size shows that the smaller the room size, the higher the received power ratio.

Then, we evaluate transmission performance using Configuration D in Table 1. The received signal is sent to the receiver detector. After that the signal is integrated during every period, then, the position of a maximum pulse after integration is defined as the pulse position of this received signal. To compute the probability of bit error, we initially find the probability of detecting a correct symbol, which is a standard technique for an orthogonal signal. Probabilities are easily expressed in terms of the common Q-function, as shown below [5]:

$$P[\text{correct symbol}] = E \left\{ 1 - Q \left(\frac{s_1 - s_2 + n_1}{\sqrt{N_o}} \right) \right\}. \quad (9)$$

$$\left[1 - Q \left(\frac{s_1 - s_3 + n_1}{\sqrt{N_o}} \right) \right] \dots \left[1 - Q \left(\frac{s_1 - s_L + n_1}{\sqrt{N_o}} \right) \right]$$

A random variable $X \sim N(u, \sigma^2)$,

$$E[Q(x)] = Q\left(\frac{\mu}{\sigma^2 + 1}\right) \quad (10)$$

Given Eq. (9), we find the probability of bit error via the following steps:

$$P[\text{symbol error}] = 1 - P[\text{correct symbol}] \quad (11)$$

$$P[\text{bit error}] \approx \frac{L/2}{(L-1)} P[\text{symbol error}] \quad (12)$$

$$= \frac{L/2}{(L-1)} \left[Q\left(\frac{s_1 - s_2}{\sqrt{2N_o}}\right) + \dots + Q\left(\frac{s_1 - s_L}{\sqrt{2N_o}}\right) \right]$$

For all simulations, 1,000,000 bits are sent and occurrences of errors are recorded. The BER was computed using Matlab for various E_b/N_o values in our studied system model. E_b/N_o is the energy per bit: N_o is the Gauss noise generator, E_b is mathematical expectation with respect to a mean of zero and variance is $\sigma^2 = N_o/2$.

After simulations, the BER curve of Gaussian pulse PPM with various duty cycles shows the Gaussian pulse with a low duty cycle yields good performance. Then because of the similar coding characteristics of OOK and 2-PPM, we investigate BER by applying various pulses to OOK and 2-PPM in diffuse and LOS channels. Fig. 8 shows that the BER performance in the LOS channel is about 2dB better than that in the diffuse channel, and the 2-PPM scheme is better than the OOK scheme. To find the

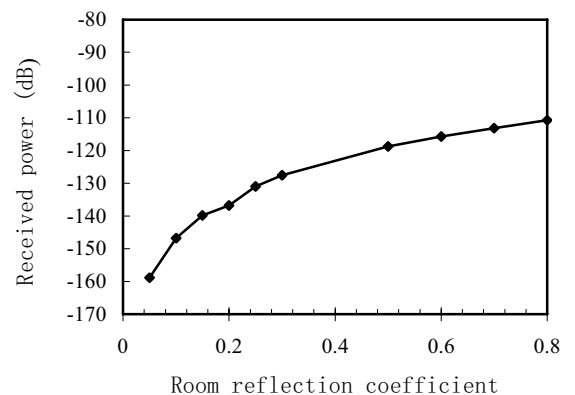


Fig. 5 Received power ratio versus room reflection coefficient.

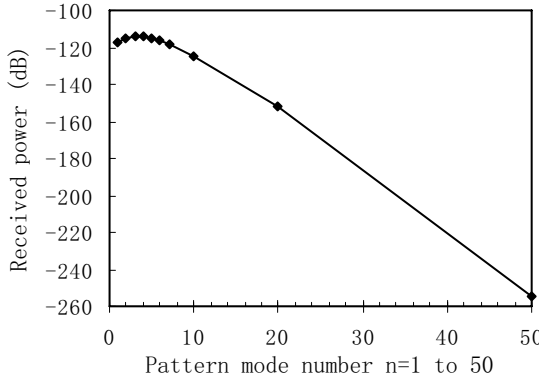


Fig. 6 Received power ratio versus pattern mode numbers.

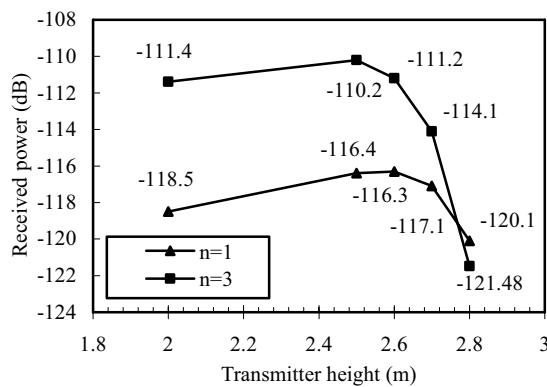


Fig. 7 Received power ratio versus transmitter height for two pattern modes ($n=1, 3$).

performance of L -PPM we evaluated the BER with various input pulse shapes for 2, 4, 8, and 16-PPM in LOS and diffuse channels. Fig. 9 shows that BER of $L=2, 4, 8$ and 16 PPM are decreasing when E_b/N_0 is increasing in a diffuse channel and 16-PPM is the best among these modulation schemes. The BER performance for LOS channel is very similar with that of the diffuse channel.

4. Conclusions

In this paper, we obtained the received power distribution according to the six configurations in Table 1, which vary with respect to transmitter and receiver positions and reflection coefficients of the indoor structure. The simulation results show that a larger reflection coefficient and smaller pattern mode number result in a higher received power level. And, the received power ratio with respect to transmitter height for two pattern modes ($n=1, 3$) were presented. Also, to find the transmission performance we presented a block diagram for a wireless optical communication system. We performed a simulation with the input Gaussian pulse, Rectangular pulse, and Practical pulse, which are applied to L -PPM and OOK, based on the impulse response of indoor channels in Configuration D of Table 1. The results show BER with respect to signal to noise ratio for various input pulse shapes in LOS and diffuse channels. We found that among the various pulses applied to OOK

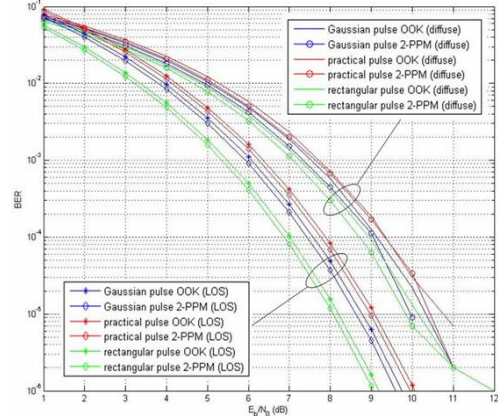


Fig. 8 BER comparison of OOK and 2-PPM in diffuse and LOS channels.

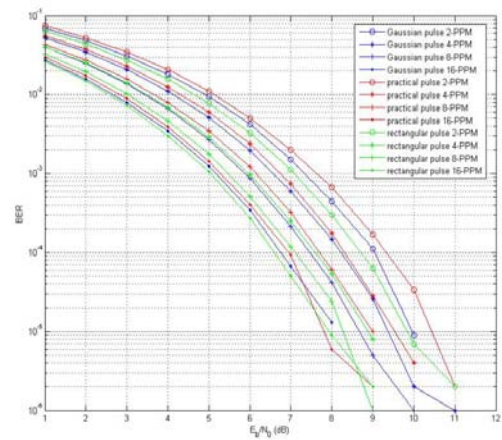


Fig. 9 L-PPM BER comparison of diffuse channel links.

and L -PPM, the BER performance of the LOS channel is better than that of the diffuse channel. BER of the Gaussian pulse in L -PPM approaches the ideal Rectangular pulse, and is also better than the Practical pulse in L -PPM. So, the Gaussian pulse in L -PPM is a modulation scheme suitable for a wireless infrared indoor channel.

References

- [1] A. Mahdy and J. Deogun, "Wireless Optical Communications: A Survey", *IEEE WCNC*, vol.4, pp. 2399-2404, March 2004.
- [2] Chuan Peng et al., "Channel Characteristics of Indoor Wireless Infrared Communication System Due to Different Transceiver Conditions", *Journal of KICS*, vol.33, no.2, pp.198-203, February 2008.
- [3] J. Barry, *Wireless Infrared Communications*, Kluwer Academic Publishers, Boston, 1994.
- [4] J. Sartthong et al., "Analysis performance of L-PPM infrared wireless communications for indoor LOS and diffuse links", *SCORED Pro.*, pp. 348-353, August 2003.
- [5] M. D. Audeh and J. M. Kahn, "Performance Evaluation of L-Pulse-Position Modulation on Non-Directed Indoor Infrared Channels", *ICC '94.*, vol.2, pp. 660-664, May 1994.